

Squaraine-Derived Rotaxanes: Highly Stable, Fluorescent Near-IR Dyes

Easwaran Arunkumar, Na Fu, and Bradley D. Smith*^[a]

Abstract: Squaraines are fluorescent, near-IR dyes with promising photo-physical properties for biomedical applications. A limitation with these dyes is their inherent reactivity with nucleophiles, which leads to loss of the chromophore. Another drawback is their tendency to form nonfluorescent aggregates in water. Both problems can be greatly attenuated by encapsulating the dye inside an amide-containing macrocycle. In other words, the squaraine becomes the thread component in a Leigh-type rotaxane, a permanently in-

terlocked molecule. Two new rotaxanes are described: an analogue with four tri(ethyleneoxy) chains on the squaraine to enhance water solubility, and a rotaxane that has an encapsulating macrocycle with transposed carbonyl groups. An X-ray crystal structure of the latter rotaxane shows that the macrocycle provides only partial protection

of the electrophilic cyclobutene core of the squaraine thread. The stabilities of each compound in various solvents, including serum, were compared with a commercially available cyanine dye. The squaraine rotaxane architecture is remarkably resistant to chemical and photochemical degradation, and likely to be very useful as a versatile fluorescent scaffold for constructing various types of highly stable, near-IR imaging probes.

Keywords: fluorescence • near-IR dyes • optical imaging • rotaxanes • squaraines

Introduction

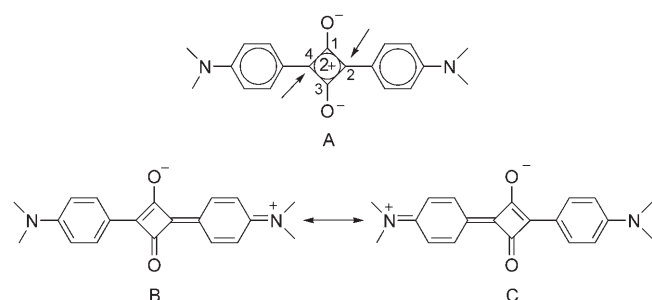
Molecular bioimaging is a rapidly developing technology that is expected to improve human health in a variety of ways, such as, the early identification of disease, facile monitoring of treatment efficacy, and acceleration of the drug-discovery process.^[1] Optical imaging using fluorescent probes is a relatively recent approach compared with more established methods like radioimaging or magnetic resonance imaging (MRI). The obvious limitation with optical imaging is restricted tissue penetration, however, it is predicted that low-energy, near-IR (NIR) radiation can pass through 10–20 cm of tissue.^[2] Major advances in tomographic three-dimensional reconstruction are also helping optical imaging to become a more feasible proposition.^[3] At pres-

ent, only a limited number of fluorescent NIR dyes are available for development into bioimaging agents, and continued progress in optical imaging will require the invention of new NIR fluorophores that exhibit improved performance in biological media. For bioimaging purposes, an ideal NIR dye should have high chemical stability, high photostability, excellent photophysical properties, insensitivity to self and biomolecular quenching, low phototoxicity, low chemical toxicity, and suitable chemical functionality for bioconjugation. Another desirable property is the ability to construct multivalent probes, that is, molecular beacons with dendritic structures consisting of a core chromophore that emits in the NIR region and a periphery of functional groups that can interact with biological targets (especially membrane-bound receptors) in a multivalent fashion. Nanoparticles and quantum dots have this sort of architecture and are under active investigation as imaging agents, but this technology is limited by slow diffusion of these relatively large probes to the target tissue, and their potential to elicit immunogenic responses *in vivo*. In addition, the constituents of quantum dots can be cytotoxic, especially upon irradiation.^[4] There is a need for small organic NIR dyes that possess the same favorable photophysical properties as quantum dots but do not have the undesirable slow diffusion or toxicity properties. At present, there is no organic NIR dye that has all of these desirable properties.^[5]

[a] Dr. E. Arunkumar, N. Fu, Prof. Dr. B. D. Smith
Department of Chemistry and Biochemistry
University of Notre Dame
Notre Dame, IN 46556 (USA)
Fax: (+1) 574-631-6652
E-mail: smith.115@nd.edu

Supporting information for this article is available on the WWW under <http://www.chemeurj.org/> or from the author. It contains additional details of the synthetic procedures, NMR spectra of **1b**, **2b**, and **3**, and a color version of Figure 1.

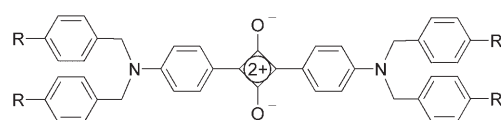
This report focuses on squaraine dyes, a family of NIR fluorophores with photophysical properties that are appropriate for many biomedical applications.^[6] Squaraines have a donor–acceptor–donor structure that can be represented by the resonance structures A, B, and C. The central cyclobutene ring is electron deficient and susceptible to nucleophilic attack at the equivalent 2 and 4 positions (see arrows in Scheme 1), which limits the use of squaraines.^[6c,f] Another



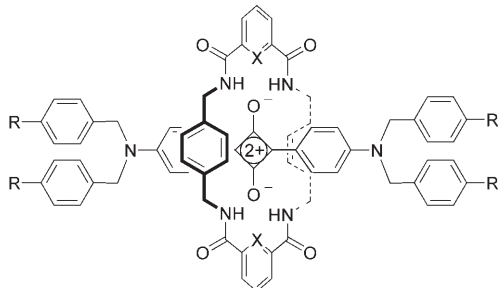
Scheme 1. Resonance structures (A, B, and C) of squaraines. The arrows show where the central cyclobutene ring is susceptible to nucleophilic attack.

drawback is their tendency to form nonfluorescent aggregates in water. We have discovered that both problems can be greatly attenuated by encapsulating the dye inside an amide-containing macrocycle.^[7] In other words, the squaraine (**1**) becomes the thread component in a Leigh-type rotaxane, a permanently interlocked molecule (**2** and **3**).^[8] Our preliminary communication on this topic included X-ray crystal structures of rotaxanes **2a** and **2c**. In both cases, the surrounding macrocycle sits perfectly over both faces of the electrophilic cyclobutene core of the squaraine thread and blocks attack at the ring by strong nucleophiles like hydroxide and thiols (see Figure 1 below).^[7] The steric protection provided by the surrounding macrocycle also explains why there is no aggregation-induced broadening of absorption or self-quenching of fluorescence. Even when aggregated, the inner squaraine chromophores are unable to get close enough to interact.

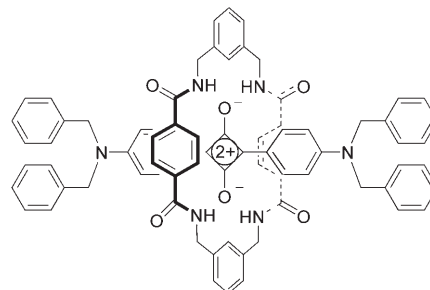
Here, we disclose two new rotaxanes, the analogue **2b**, which contains four tri(ethyleneoxy) chains that greatly enhance water solubility and allow characterization in biological media, and rotaxane **3**, which is an isomer of **2a** that differs by having an encapsulating macrocycle with transposed carbonyl groups. We compare the stabilities of these compounds in various solvents, including serum, with the commercially available cyanine dye **4**. We find that the squaraine rotaxane architecture of **2** is remarkably resistant to chemical and photochemical degradation, and likely to be very useful as a versatile fluorescent scaffold for constructing various types of highly stable, NIR imaging probes.



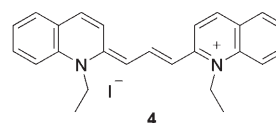
1a: R = H
1b: R = OCH₂(CH₂-O-CH₂)₂CH₂-OCH₃



2a: X = CH, R = H
2b: X = N, R = OCH₂(CH₂-O-CH₂)₂CH₂-OCH₃
2c: X = N, R = H



3



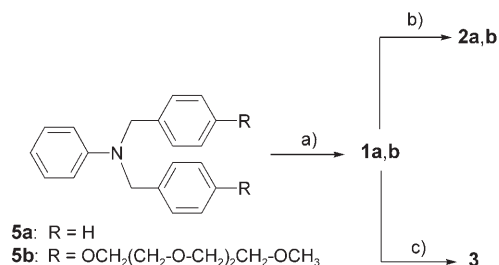
4

Results and Discussion

Molecular designs: Our preliminary studies showed that the pyridyl-containing macrocycle in rotaxane **2c** protected the squaraine thread slightly better than the isophthalamide-containing macrocycle in analogue **2a**.^[7] X-ray crystal structures indicated that the pyridyl-containing macrocycle forms internal hydrogen bonds between the pyridyl nitrogen and the two adjacent amide NH residues, which contracts the macrocycle and wraps it more tightly around the cyclobutene core of the squaraine thread. The limited solubility of **2c** in mixed aqueous/organic solvents prevented a quantitative evaluation of its long-term stability; therefore, rotaxane **2b**, with four peripheral tri(ethyleneoxy) chains attached to the squaraine, was designed as a more water-soluble analogue. At present, most optical-imaging studies employ cyanine dyes.^[1,2] Thus, it was of interest to compare the stability of **2b** with a representative cyanine dye. Compound **4** was chosen for this comparison primarily because of its commercial availability and its similar absorption/emission wavelengths.

The other new molecular design that is reported here is rotaxane **3**, an isomer of **2a** that differs in the location of the four carbonyl groups on the surrounding macrocycle. Rotaxane **2a** employs a normal Leigh-type macrocycle with electron-rich 1,4-xylylene units; whereas, the macrocycle in **3** incorporates electron-deficient 1,4-phthaloyl units.^[9] The goal was to determine if rotaxane **3** can be synthesized, and if so, to compare its structure and photochemical properties with isomer **2a**. In other words, what are the effects of “reversing” the aromatic electron density in the surrounding macrocycle?

Synthesis and structure: Rotaxanes **2** and **3** were prepared by using the templated amide cyclization chemistry developed by Leigh and co-workers.^[8,9] Squaraine dyes **1a,b** were obtained by reacting aniline derivatives **5a,b** and squaric acid under azeotropic distillation conditions (Scheme 2).^[10] The purified dyes were treated with an ap-



Scheme 2. Conditions: a) squaric acid, benzene/*n*-butanol (2:1), reflux; b) 2,6 pyridinedicarbonyl dichloride or isophthaloyl dichloride, *p*-xylylenediamine, TEA, CHCl₃; c) terephthaloyl chloride, *m*-xylylenediamine, TEA, CHCl₃.

propriate mixture of diacid dichloride and xylylenediamine under high-dilution conditions to consistently give rotaxanes **2a** and **2b** in yields of 30–35% and **3** in 9% yield. Although these yields are fairly low, it should be remembered that in each case the one-pot reaction forms four covalent bonds and captures five molecular components. Our observation that the reaction yield for **3** is significantly less than that for isomeric architecture **2** agrees with the reactivity trend reported by Leigh.^[9]

The X-ray crystal structure of **3** is illustrated in Figure 1, along with the previously reported structure for **2a**.^[7] In both cases, the four macrocyclic NH residues form bifurcated hydrogen bonds with the two squaraine oxygen atoms. In addition to the expected variations in macrocycle conformation produced by the different conjugation patterns, there is a major difference in macrocycle orientation relative to the squaraine thread. In the case of **2a**, the two 1,4-xylylene units are positioned exactly over both faces of the central, electron-deficient cyclobutene ring, whereas the equivalent 1,4-phthaloyl units in **3** are staggered such that they avoid the central cyclobutene ring and partially overlap with the adjacent electron-rich, squaraine anilinium rings. It appears that an important structural factor with both rotaxane archi-

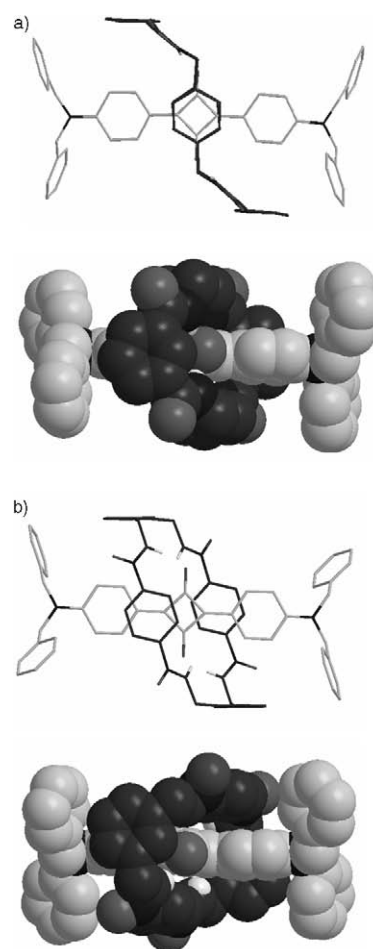


Figure 1. X-ray crystal structures of a) **2a** (reprinted with permission from reference ^[7]; copyright (2005) American Chemical Society) and b) **3**. Both structures are shown from two views, side and top. Intramolecular hydrogen-bond lengths [Å] and angles [°] in **2a** are 3.05, 165; 2.80, 163; 3.02, 163; 2.76, 164, and in **3** are 3.04, 139; 3.16, 152. A color version of this picture is available in the Supporting Information.

tectures is the maximization of favorable, aromatic stacking interactions between the surrounding macrocycle and the squaraine thread. Unlike rotaxane **2a**, isomer **3** is poorly soluble in weakly polar solvents, which prohibited attempts to conduct low-temperature NMR spectroscopic studies. The difference in rotaxane solubilities is surprising because in both cases, the solid-state structures show all four NH residues involved in internal hydrogen bonds.

Photophysical properties: As expected, rotaxane **2b**, with its four tri(ethyleneoxy) chains, exhibits improved solubility in aqueous systems compared with **2a** and **2c**, but nonetheless, it is not completely water soluble. For example, a solution of **2b** (5.8 μM) in 100% aqueous solution can be prepared by using sonication, but it precipitates after sitting overnight, which hinders studies of long-term stability. To circumvent this precipitation problem, all measurements in aqueous solution included 20% THF.

The absorption and emission properties for compounds **1–4** in different solvent mixtures are listed in Table 1. In dry THF, all of the squaraine derivatives absorb strongly at

Table 1. The absorption and emission properties for compounds **1–4** in different solvent mixtures.

Solvent	Compound	λ_{abs}	$\log \epsilon$	$\lambda_{\text{em}}^{[a]}$	$\Phi_{\text{f}}^{[b]}$
THF	1a	631	5.7	650	0.61
	1b	636	5.7	656	0.67
	2b	644	5.7	667	0.66
	3	644	5.7	672	0.61
	4	610, 565	4.3	628	0.03
water/THF (4:1)	1a	737, 540	5.6	671	0.0001
	1b	637	5.7	677	0.27
	2b	653	5.7	681	0.38
	3	655	5.7	678	0.002
	4	603, 560	4.7	622	0.003
serum/THF (4:1)	2b	653	5.7	680	0.34
	4	605, 561	4.7	628	0.003

[a] Solutions were excited at 580 nm and emission monitored in the region 600–750 nm for estimating Φ_{f} . [b] Fluorescence quantum yields were determined using 4,4-bis(*N,N*-dimethylamino)phenyl]squaraine dye as the standard ($\Phi_{\text{f}}=0.7$ in CHCl_3), error limit $\pm 5\%$.

around $\lambda_{\text{abs}}=640$ nm ($\log \epsilon \approx 5.7$) and emit at around $\lambda_{\text{em}}=660$ nm with high quantum yields in the range of $\Phi_{\text{f}}=0.61$ –0.67. In comparison, the cyanine dye **4** exhibits an absorption maximum at $\lambda_{\text{abs}}=610$ nm and a shoulder band at $\lambda_{\text{abs}}=565$ nm, indicating that the dye forms a nonfluorescent H-type aggregate (head-to-head stacking), which explains why the fluorescence quantum yield is only 0.03.^[11] In the more polar solvent mixture of water/THF (4:1) the absorption and emission maxima of the squaraine derivatives are red-shifted by about 10–15 nm, which is in accordance with previous theoretical and experimental results.^[12] A notable observation is the high fluorescence quantum yields for squaraine **1b** and related rotaxane **2b** even in aqueous solution, whereas, squaraine **1a** forms nonfluorescent aggregates. Thus, the presence of the four tri(ethyleneoxy) chains appears to greatly diminish dye aggregation.^[13] The susceptibility of rotaxane **2b** to biological quenchers was evaluated by addition of an excess of tryptophan (30 mM), which reduced the fluorescence intensity by a negligible amount.^[14] Thus, rotaxane **2b** is predicted to be quite resistant to quenching in biological media.

Chemical and photochemical stability: Previously, we reported that squaraine **1a** is susceptible to nucleophilic attack by thiols, whereas, rotaxane **2a** is quite stable for months under the same conditions.^[7] Here, we expand the stability profile by first describing hydrolytic bleaching experiments with squaraine derivatives **1–3** at different values of pH and temperature. These bench-top studies were conducted in the presence of laboratory lights.

The pH study monitored the change in the absorption and emission spectra of each dye in water/THF (4:1) over a pH range of 1.5 to 12. The chromophores of squaraine **1b** and rotaxane **3** were readily destroyed in basic solution but were

moderately stable in acid. In contrast, solutions of rotaxane **2b** were completely stable for days over the entire pH window. The enhanced stability of **2b** relative to **3** is notable and is consistent with the idea that the surrounding macrocycle sterically hinders nucleophilic attack at the central cyclobutene core of the squaraine thread. The macrocycle in **3** is less effective because it leaves the cyclobutene unit partially exposed.

The temperature study produced essentially the same stability trend. As shown in Figure 2, the hydrolytic decomposition of cyanine **4**, and especially squaraine **1b**, increases significantly with temperature; whereas, rotaxane **2b** is quite stable at 60 °C and pH 7.

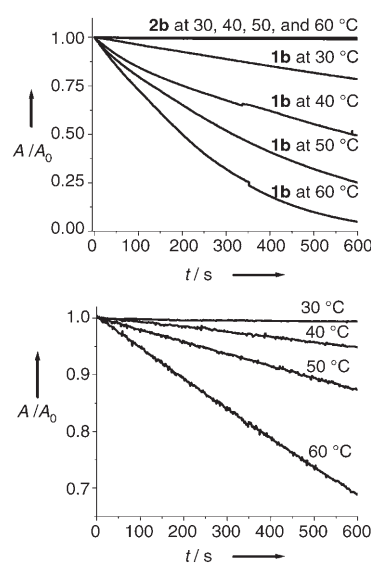


Figure 2. Time-dependant variation in absorption maxima of **1b** and **2b** (top) and **4** (bottom) in water/THF (4:1) with increasing temperature. A is the absorbance at time t and A_0 is the initial absorbance.

An important technical problem with fluorescence imaging is photobleaching, which leads to loss of signal. The susceptibility of compounds **1–4** to photobleaching was measured in the following way. In each case, a quartz cuvette containing a solution of dye in water/THF (4:1) was exposed to light irradiating from a 60 W tungsten filament bulb at a distance of 30 cm. The changes in the absorption and emission spectra for the separate samples are shown in Figure 3. The rotaxane **2b** was essentially unchanged over a five hour irradiation period; whereas, compounds **1b**, **3**, and **4** underwent extensive bleaching. The resulting decay curves were fitted to a first-order kinetic model and the following first-order rate constants were extracted: **1b**, $8.54 \times 10^{-2} \text{ min}^{-1}$; **3**, $3.621 \times 10^{-2} \text{ min}^{-1}$; **4**, $7.57 \times 10^{-3} \text{ min}^{-1}$. These decay rates are only about two times faster than the rates obtained in the presence of weak laboratory lights, which indicates that strong irradiation does not greatly accelerate dye bleaching. The data further demonstrate that the steric protection provided by the surrounding macrocycle in rotaxane **2b** is much greater than that provided by the macrocycle in rotaxane **3**.

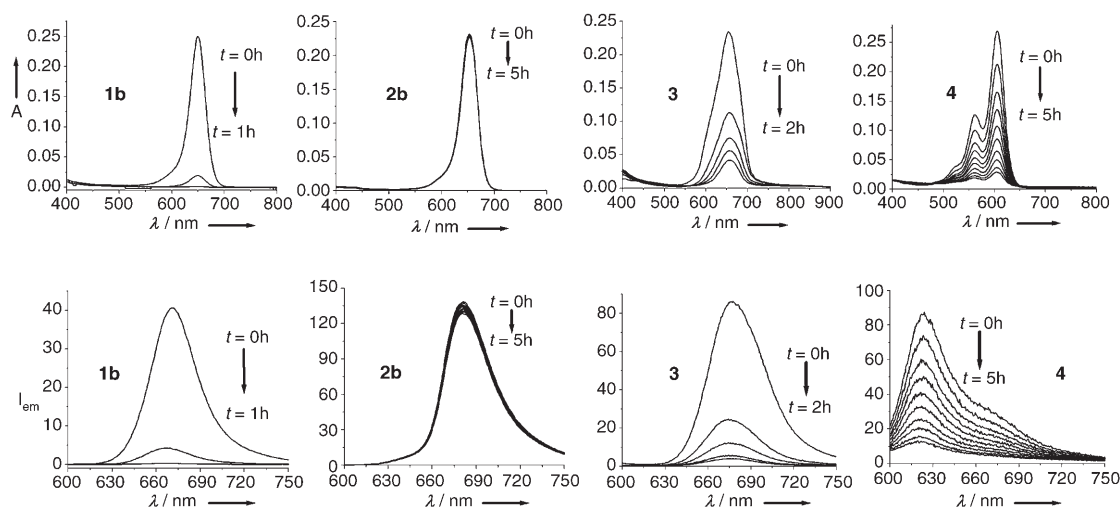


Figure 3. Change in absorption (top) and emission (bottom) spectra for solutions (5.8 μM) of **1b**, **2b**, **3**, and **4** in water/THF (4:1) mixture exposed to a 60 W bulb light. Measurements were recorded at 30 min intervals.

Stability in serum solution: As a final and more extreme in vitro test of biological stability, the decomposition of compounds **1–4** was monitored in solutions containing serum. Separate samples of each dye were prepared in a solvent mixture of serum/THF (4:1) in which the serum was an 8% aqueous fetal bovine serum solution. The absorbance and fluorescence spectra for each sample was monitored over time. In the cases of squaraine **1b** and rotaxane **3**, the chromophores were destroyed within seconds after sample preparation (presumably due to attack by the biomolecular nucleophiles present in the serum); whereas, the color associated with cyanine **4** disappeared over a few minutes. In dramatic contrast, the absorption and emission spectra for rotaxane **2b** were unaltered after standing for several days on a laboratory bench top.

Conclusion

Squaraines have promising photophysical properties as fluorescent NIR dyes, but their utility in optical bioimaging applications is limited by their susceptibility to chemical attack by nucleophilic biomolecules. Permanent encapsulation of a squaraine dye, as the thread component in a Leigh-type rotaxane, provides tremendous chemical stabilization as seen with squaraine rotaxane **2b**. This compound can sit on the bench top, in the presence of serum, for many weeks without apparent degradation, which makes it one of the most stable, organic NIR dyes ever reported. The rotaxane's enhanced stability is due to the surrounding macrocycle that sits perfectly over both faces of the electrophilic cyclobutene core of the squaraine thread and blocks nucleophilic attack. The steric protection provided by the macrocycle depends on its precise molecular structure, which controls its orientation relative to the encapsulated squaraine. For example, the macrocycle in rotaxane **3** does not perfectly cover the central cyclobutene core of its squaraine thread and so the dye

is more susceptible to bleaching through nucleophilic attack. Future synthetic efforts will attempt to prepare analogues of **2b** that can be converted into practical, useful fluorescent bioconjugates.

Experimental Section

Measurements: ^1H and ^{13}C NMR spectra were recorded by using Varian Unity Plus spectrometers. Fast atom bombardment (FAB) mass spectra (MS) were recorded on a JEOL AX 505 HA instrument.

Procedure to synthesize squaraine dyes (1a,b): The dibenzylaniline derivative **5a** or **5b** (0.67 mmol) was added to a solution of squaric acid (38 mg, 0.34 mmol) in a mixture of *n*-butanol (15 mL) and benzene (30 mL) in a 100 mL round-bottomed flask equipped with Dean–Stark apparatus. The reaction mixture was left at reflux, while the water formed in the reaction mixture was trapped in the Dean–Stark apparatus. After 12 h the deep-green reaction mixture was concentrated to remove the solvent and the crude product was precipitated by adding hexane (30–40 mL). After filtering, the product was washed several times with hexane to give the dark green squaraine dye, which was further purified by using column chromatography over silica gel with MeOH/CHCl₃ (1:19) as the eluent.

Dye 1a:^[7a] Yield 35%; ^1H NMR (500 MHz, CDCl₃, TMS): δ = 4.80 (s, 8H), 6.87 (d, J = 9 Hz, 4H), 7.19–7.38 (m, 20H), 8.36 ppm (d, J = 9 Hz, 4H); ^{13}C NMR data were not acquired because of poor solubility; FAB-MS (NBA matrix): m/z : 626 [$M+H$]⁺.

Dye 1b: Yield 37%; ^1H NMR (300 MHz, CDCl₃, TMS): δ = 3.37 (s, 12H; -OCH₃), 3.55 (t, J = 4.5 Hz, 8H; -OCH₂), 3.64–3.75 (m, 24H; -OCH₂), 3.86 (t, J = 4.8 Hz, 8H; -OCH₂), 4.12 (t, J = 4.8 Hz, 8H; -OCH₂), 4.69 (s, 8H; -Ph-CH₂), 6.89 (d, J = 8.7 Hz, 12H; aromatic), 7.09 (d, J = 8.7 Hz, 8H; aromatic), 8.38 ppm (d, J = 9.3 Hz, 4H; aromatic); ^{13}C NMR (150 MHz, CDCl₃, TMS): δ = 53.2, 59.1, 67.5, 69.7, 70.6, 70.7, 70.8, 71.9, 113.1, 115.2, 120.7, 127.8, 127.9, 133.6, 155.1, 158.4, 183.1, 189.9 ppm; FAB-MS (NBA matrix): m/z : 1274 [$M+H$]⁺.

Procedure to synthesize squaraine rotaxanes 2a–c and 3: Clear solutions of the corresponding diacid dichloride (1.28 mmol) and diamine (1.28 mmol) in chloroform (5 mL) were simultaneously added dropwise, by using a mechanical syringe pump (kd Scientific) apparatus, over five hours to a stirred solution of **1** (0.32 mmol) and triethylamine (TEA; 3.2 mmol) in CHCl₃ (40 mL). After stirring overnight, the reaction mixture was filtered through a pad of Celite to remove any polymeric mate-

rial, and the resulting crude product was subjected to chromatography by using a silica column and a mixture of methanol/chloroform (1:19) as the eluent.

Rotaxane 2a:^[7a] Yield 30%; TLC: $R_f=0.5$ (methanol/chloroform 1:19); ¹H NMR (500 MHz, CDCl₃, TMS): $\delta=4.38$ (d, $J=5$ Hz, 8H; -Ph-CH₂ (wheel)), 4.79 (s, 8H; -Ph-CH₂ (thread)), 6.47 (d, $J=9$ Hz, 4H; thread), 6.66 (s, 8H; wheel), 7.16 (d, $J=8$ Hz, 8H; thread), 7.37 (t, $J=7$ Hz, 4H; thread), 7.41 (t, $J=8$ Hz, 8H; thread), 7.51 (t, $J=8$ Hz, 2H; wheel), 7.69 (d, $J=10$ Hz, 4H; thread), 8.06 (t, $J=10$ Hz, 4H; -NH), 8.20 (d, $J=10$ Hz, 4H; wheel), 9.22 ppm (s, 2H; wheel); ¹³C NMR (125 MHz, CDCl₃, TMS): $\delta=44.1, 54.6, 113.2, 118.7, 124.5, 126.4, 128.2, 129.1, 129.2, 129.3, 131.6, 133.1, 133.9, 135.2, 136.4, 155.3, 166.0, 183.1, 184.9$; FAB-MS (NBA matrix): $m/z: 1158 [M+H]^+$.

Rotaxane 2b: Yield 34%; TLC: $R_f=0.3$ (methanol/chloroform 1:19); ¹H NMR (300 MHz, CDCl₃, TMS): $\delta=3.37$ (s, 12H; -OCH₃), 3.55 (t, $J=4.4$ Hz, 8H; -OCH₂), 3.64–3.75 (m, 24H; -OCH₂), 3.89 (t, $J=4.8$ Hz, 8H; -OCH₂), 4.17 (t, $J=4.8$ Hz, 8H; -OCH₂), 4.50 (d, $J=5.7$ Hz, 8H; -Ph-CH₂ (wheel)), 4.56 (s, 8H; -Ph-CH₂ (thread)), 6.28 (d, $J=9.6$ Hz, 4H; thread), 6.56 (s, 8H; wheel), 6.92 (d, $J=9$ Hz, 8H; thread), 6.99 (d, $J=8.7$ Hz, 8H; thread), 8.02 (t, $J=7.8$ Hz, 2H; wheel), 8.07 (d, $J=9.3$ Hz, 4H; thread), 8.40 (d, $J=8.1$ Hz, 4H; wheel), 9.89 ppm (t, $J=5.9$ Hz, 4H; -NH); ¹³C NMR (150 MHz, CDCl₃, TMS): $\delta=43.2, 53.4, 59.0, 67.5, 69.7, 70.5, 70.6, 70.8, 71.9, 112.5, 115.1, 119.6, 125.1, 127.5, 127.8, 128.9, 133.5, 136.6, 138.6, 149.3, 154.8, 158.5, 163.4, 184.9, 185.5$ ppm; FAB-MS (NBA matrix): $m/z: 1810 [M+H]^+$.

Rotaxane 2c:^[7a] Yield 30%; TLC: $R_f=0.5$ (methanol/chloroform 1:19); ¹H NMR (500 MHz, CDCl₃, TMS): $\delta=4.50$ (d, $J=6$ Hz, 8H; -Ph-CH₂ (wheel)), 4.67 (s, 8H; -Ph-CH₂ (thread)), 6.26 (d, $J=9$ Hz, 4H; thread), 6.66 (s, 8H; wheel), 7.11 (d, $J=9$ Hz, 8H; thread), 7.34–7.41 (m, 20H; thread), 7.99 (t, $J=8$ Hz, 4H; wheel), 8.06 (d, $J=9$ Hz, 4H; thread), 8.37 (d, $J=8$ Hz, 4H; wheel), 9.86 ppm (t, $J=6$ Hz, 4H; -NH); ¹³C NMR (125 MHz, CDCl₃, TMS): $\delta=43.4, 54.5, 112.7, 120.0, 125.3, 126.6, 128.2, 129.0, 129.4, 133.8, 135.7, 136.9, 138.7, 149.4, 155.1, 163.6, 185.0, 186.3$; FAB-MS (NBA matrix): $m/z: 1159 [M+H]^+$.

Rotaxane 3: Yield 9%; TLC: $R_f=0.5$ (methanol/chloroform 1:19); ¹H NMR (800 MHz, DMSO, TMS): $\delta=4.43$ (d, $J=5.6$ Hz, 8H; -Ph-CH₂ (wheel)), 4.80 (s, 8H; -Ph-CH₂ (thread)), 6.23 (d, $J=8.8$ Hz, 4H, thread), 6.93 (s, 8H; wheel), 6.97 (t, $J=7.6$ Hz, 2H; wheel), 7.2 (d, $J=8$ Hz, 4H; wheel), 7.24–7.26 (m, 12H; thread), 7.35 (t, $J=7.2$ Hz, 4H; thread), 7.43 (t, $J=7.6$ Hz, 4H; thread), 7.7 (s, 2H; wheel), 8.28 ppm (t, $J=6$ Hz, 4H; -NH); ¹³C NMR data were not acquired because of poor solubility; FAB-MS (NBA matrix): $m/z: 1158 [M+H]^+$.

X-ray crystallographic structure determinations

Rotaxane 3: Crystallization was carried out in dimethylformamide (DMF)/diisopropyl ether (1:1). Molecular formula = C₈₈H₉₂N₁₀O₁₀; $M_r=1449.72$; crystal size = $0.43 \times 0.11 \times 0.06$ mm³; monoclinic; space group P2₁/c; translucent blue needles; $a=9.8115(4)$, $b=16.4125(6)$, $c=24.0231(10)$ Å; $\beta=99.994(3)^\circ$; $V=3809.8(3)$ Å³; $Z=2$; $\rho_{\text{calcd}}=1.264$ mg m⁻³. Crystals were examined under a light hydrocarbon oil. The crystal was affixed to a thin glass fiber mounted atop a tapered copper mounting pin and transferred to the 100 K nitrogen stream of a Bruker APEX diffractometer equipped with an Oxford Cryosystems 700 series low-temperature apparatus. Cell parameters were determined with CellNow by using reflections harvested from three sets of twenty 0.3° ω scans. The orientation matrix derived from this was passed to COSMO to determine the optimum data-collection strategy. Average fourfold redundancy was achieved by using four ω scan series. Data were measured to 0.80 Å. Cell parameters were refined by using 5480 reflections with $I=10\sigma(I)$ and $2.12^\circ=\sigma=23.12^\circ$ harvested from the entire data collection. In total, 70216 reflections were measured, 12323 unique, 7395 observed, $I>2\sigma(I)$. All data were corrected for Lorentz and polarization effects and runs were scaled by using TWINABS. The structure was solved by using data from the dominant component and refined against data from all three components. The scale factors for the second and third components are 0.3274(14) and 0.1938(14), respectively. The asymmetric unit contains a 1/2 molecule each of the squaraine and macrocycle. In addition, there are two molecules of DMF. The complete structure is generated by inversion. Hydrogen atoms were placed at calculated geometries and allowed

to ride on the positions of the parent atoms. All non-hydrogen atoms were refined with parameters for anisotropic thermal motion. There were no significant peaks in the final difference map; the largest peak = $0.26 \text{ e} \text{ \AA}^{-3}$. The deepest hole was of similar magnitude, $0.25 \text{ e} \text{ \AA}^{-3}$.

CCDC-297976 (3) contains the supplementary crystallographic data for this paper. This data can be obtained free of charge from the Cambridge Crystallographic Data Centre via www.ccdc.cam.ac.uk/data_request/cif.

Acknowledgements

This work was supported by the National Institutes of Health (USA), Philip Morris USA Inc., and Philip Morris International. The X-ray diffraction instrumentation was supported by NSF award CHE-0443233.

- [1] a) V. Marx, *Chem. Eng. News* **2005**, July 25, 25–34; b) F. A. Jaffer, R. Weissleder, *JAMA J. Am. Med. Assoc.* **2005**, *293*, 855–862; c) F. A. Jaffer, R. Weissleder, *Circ. Res.* **2004**, 433–445.
- [2] C. Tung, Y. Lin, W. Moon, R. Weissleder, *ChemBioChem* **2002**, *3*, 784–786.
- [3] E. M. Sevick-Muraca, J. P. Houston, M. Gurfinkel, *Curr. Opin. Chem. Biol.* **2002**, *6*, 642–650.
- [4] D. J. Bharli, D. W. Lucey, H. Jayakumar, H. E. Pudavar, P. N. Prasad, *J. Am. Chem. Soc.* **2005**, *127*, 11364–11371.
- [5] E. Arunkumar, C. C. Forbes, B. D. Smith, *Eur. J. Org. Chem.* **2005**, 4051–4059.
- [6] a) S. Das, K. G. Thomas, M. V. George in *Organic Photochemistry* (Eds.: V. Ramamurthy, K. S. Schanze), Marcel Dekker, New York, **1997**, pp. 467–517; b) M. Emmelius, G. Pawlowski, H. W. Vollmann, *Angew. Chem.* **1989**, *101*, 1475; *Angew. Chem. Int. Ed. Engl.* **1989**, *28*, 1445–1471; c) A. Ajayaghosh, E. Arunkumar, J. Daub, *Angew. Chem.* **2002**, *114*, 1844–1847; *Angew. Chem. Int. Ed.* **2002**, *41*, 1766–1769; d) D. Ramaiah, A. Joy, N. Chandrasekhar, N. V. Eldho, S. Das, M. V. George, *Photochem. Photobiol.* **1997**, *65*, 783–790; e) J. V. Ros-Lis, B. García, D. Jiménez, R. Martínez-Máñez, F. Sancenón, J. Soto, F. Gonzalvo, M. C. Valdecabres, *J. Am. Chem. Soc.* **2004**, *126*, 4064–4065; f) J. V. Ros-Lis, R. Martínez-Máñez, J. Soto, *Chem. Commun.* **2002**, 2248–2249.
- [7] a) E. Arunkumar, C. C. Forbes, B. C. Noll, B. D. Smith, *J. Am. Chem. Soc.* **2005**, *127*, 3288–3289; b) Other examples of rotaxanes with dyes as thread components include: S. Anderson, H. L. Anderson, *Angew. Chem.* **1996**, *108*, 2075–2078; *Angew. Chem. Int. Ed. Engl.* **1996**, *35*, 1956–1959; F. Cacialli, J. S. Wilson, J. J. Michels, C. Daniel, C. Silva, R. H. Friend, N. Severin, P. Samori, J. P. Rabe, M. J. O'Connell, P. N. Taylor, H. L. Anderson, *Nat. Mater.* **2002**, *1*, 160–164, and references therein; S. A. Haque, J. S. Park, M. Srinivasarao, J. R. Durrant, *Adv. Mater.* **2004**, *16*, 1177–1181; c) For a recent review of methods to stabilize dyes by molecular encapsulation, see ref. [5].
- [8] a) D. A. Leigh, A. Murphy, J. P. Smart, A. M. Z. Slawain, *Angew. Chem.* **1997**, *109*, 752–756; *Angew. Chem. Int. Ed. Engl.* **1997**, *36*, 728–732; b) F. G. Gatti, D. A. Leigh, S. A. Nepogodiev, A. M. Z. Slawain, S. J. Teat, J. K. Y. Wong, *J. Am. Chem. Soc.* **2001**, *123*, 5983–5989; c) D. A. Leigh, J. K. Y. Wong, F. Dehez, F. Zerbetto, *Nature* **2003**, *424*, 174–179.
- [9] D. A. Leigh, A. Venturini, A. J. Wilson, J. K. Y. Wong, F. Zerbotto, *Chem. Eur. J.* **2004**, *10*, 4960–4969.
- [10] A. H. Schmidt, *Synthesis* **1980**, 961–994.
- [11] a) T. Katoh, Y. Inagaki, R. Okazaki, *J. Am. Chem. Soc.* **1998**, *120*, 3623–3628; b) L. Lu, R. J. Lachicotte, T. L. Penner, J. Perlstein, D. G. Whitten, *J. Am. Chem. Soc.* **1999**, *121*, 8146–8156; c) E. N. Ushakov, S. P. Gromov, O. A. Fedorova, Y. V. Pershina, M. V. Alifimov, F. Barigelletti, L. Flamigni, V. Balzani, *J. Phys. Chem. A* **1999**, *103*, 11188–11193; d) F. Würthner, S. Yao, *Angew. Chem.* **2000**, *112*, 2054–2057; *Angew. Chem. Int. Ed.* **2000**, *39*, 1978–1981; e) S. Zeena, K. G. Thomas, *J. Am. Chem. Soc.* **2001**, *123*, 7859–7865.

- [12] a) R. W. Bigelow, H. J. Freund, *Chem. Phys.* **1986**, *107*, 159–174;
b) K. Y. Law, *J. Photochem. Photobiol. A* **1994**, *84*, 123–132.
- [13] K. T. Arun, D. Ramaiah, *J. Phys. Chem. A* **2005**, *109*, 5571–5578.
- [14] N. Marmé, J.-P. Knemeyer, M. Sauer, J. Wolfrum, *Bioconjugate Chem.* **2003**, *14*, 1133–1139.

Received: December 9, 2005
Published online: March 31, 2006